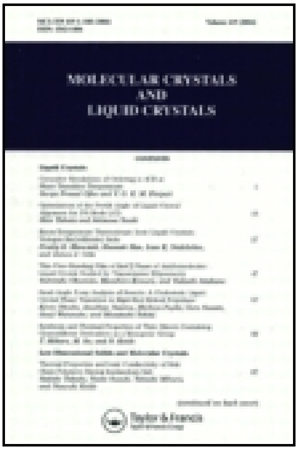

Molecular Crystals and Liquid Crystals Science and Technology. Section A. Molecular Crystals and Liquid Crystals

Publication details, including instructions for authors and subscription information:
http://www.tandfonline.com/loi/gmcl19

Metal Coordination Complexes Composed of Photo-Electrochemically Active Ligands

Michio M. Matsushita [a] [b], Masanari Morikawa [a], Tadashi Kawai [a] & Tomokazu Iyoda [a]

[a] Department of Applied Chemistry, Graduate School of Engineering, Tokyo Metropolitan University, Minami-Ohsawa, Hachioji, Tokyo, 192-0397, Japan

[b] PRESTO, JST

Version of record first published: 24 Sep 2006

To cite this article: Michio M. Matsushita, Masanari Morikawa, Tadashi Kawai & Tomokazu Iyoda (2000): Metal Coordination Complexes Composed of Photo-Electrochemically Active Ligands, Molecular Crystals and Liquid Crystals Science and Technology. Section A. Molecular Crystals and Liquid Crystals, 343:1, 87-96

To link to this article: http://dx.doi.org/10.1080/10587250008023508

Mol. Cryst. and Liq. Cryst., 2000, Vol. 343, pp. 87-96
Reprints available directly from the publisher
Photocopying permitted by license only

Published by license under the
Gordon and Breach Science Publishers imprint.
Printed in Malaysia

Metal Coordination Complexes Composed of Photo-Electrochemically Active Ligands

MICHIO M. MATSUSHITA[ab], MASANARI MORIKAWA[a],
TADASHI KAWAI[a] and TOMOKAZU IYODA[a*]

[a]*Department of Applied Chemistry, Graduate School of Engineering, Tokyo Metropolitan University, Minami-Ohsawa, Hachioji, Tokyo 192–0397, Japan and* [b]*PRESTO, JST*

N-arylpyridinium molecules, 4,6-bis(4,4'-bipyridine-1-yl)-pyrimidine (**1**) and 3,6-bis(4,4'-bipyridine-1-yl)-pyridazine (**2**) and 3-pyridylviologen (**3**) were designed and synthesized as photoelectrochemically active ligands for coordination polymer assemblies with various ions. Their two-step reduction processes involving ion-radicals generation were observed in both electrochemical and photochemical processes. The photochemical ionradical formation in **1**–**3** were observed in the solid state. The magnetic behavior of Cu complex of **3** after light irradiation showed the antiferromagnetic interaction between photochemically generated ionradical and Cu spins.

Keywords: light-induced electrochromism; conjugated molecular assembly; viologen; N-arylpyridinium; spin manipulation

INTRODUCTION

Photochemically active molecules, such as azobenzenes, spiropyranes, and diarylethenes, have been investigated widely as key compounds for novel photofunctional materials.[1] Although these molecules show the clear and reversible photochromism in the solution driven by light irradiation at two independent wavelengths and through exothermic back reaction in the dark, the question arises whether or not they exhibit the similar photochromic features in solid state. Because the photochromic processes accompany considerable changes in both electronic and geometric structures which may be limited in the solid state. This is one of the crucial disadvantages of these photochromic molecular units fabricated into the functional molecular

---

* (mmm@ecomp.metro-u.ac.jp)

assemblies in the solid state. On the other hand, viologens have been investigated as electrochromic materials, in which one-electron reduced ionradical species shows the characteristic blue color.[2] The viologens also show the light-induced electrochromism, resulted from photo-induced electron transfer from appropriate electron donors, such as chloride ion, *p*-toluenesulfonate ion, and alcohol.[3] Recently, we investigated the photoelectrochemical behavior of π-conjugated viologen dimers, connected with heteroaromatic linkers, and demonstrated both electro- and photochemical four-step reduction processes in the solid state.[4] Of much interest is the spin multiplicity of their two-electron reduced states. The two-electron reduced state of the 4,6-pyrimidinylene linked meta-type dimer was identified to be a triplet diradical in the ground state, whereas that of 3,6-pyridazinylene linked para-type dimer has a closed-shell structure through quinoid formation. The four-step redox processes result from the strong correlation of two-step redox behavior per one viologen moiety. The difference in the spin multiplicity of both two-electron reduced states results from the difference in spin exchange interaction via heteroaromatic linkers whether the substitution type is meta or para, similar to well-known 1,3- and 1,4-phenylene linkers. Thus, these features are due to the π-conjugative combination of two viologen moieties through heteroaromatic linkers. When the further extension is achieved by introduction of strong interactions, the novel photoelectrochemically active property depends on the electronic properties of viologen and their assembly structure. To this purpose, we considered to utilize the coordination bond to assemble the viologen molecules and extend the conjugated path through appropriate metal ions and metal complexes. Along this line, we designed three types of N-aryl pyridiniums and viologen derivatives, bearing pyridyl moieties for coordination bond. Pyridyl-pyridinium-type ligands, **1** and **2**, have meta-type 4,6-pyrimidinylene and para-type 3,6-pyridazinylene linkers, respectively, similar to the above viologen derivatives.

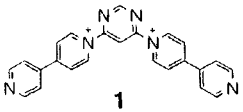

1

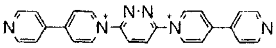

2

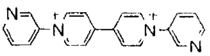

3

In this paper, we report the syntheses and photoelectrochemical behaviors of the redox active ligands **1-3**. The complexation with various metal ions and the magnetic interaction between photochemically generated ionradical and the assembled metal ion through coordination bond are discussed.

RESULTS AND DISCUSSION

Preparation of N-arylpyridinium ligands

The *N*-arylpyridinium ligands were prepared as described in Scheme 1. The pyridylpyridinium-type ligands (**1**, **2**) were prepared by nucleophilic reaction of 4,4'-bipyridine with 4,6-dichloropyrimidine or 3,6-dichlropyridazine. The viologen-type ligand (**3**) was prepared by the exchange reaction between 2,4-dinitrophenyl viologen and 3-aminopyridine.[5] Their counter anions were quantitatively exchanged to hexafluorophosphate and perchlorate ions by re-precipitation from their aqueous solutions with ammonium hexafluorophosphate and tetrabutyl ammonium perchlorate, respectively.

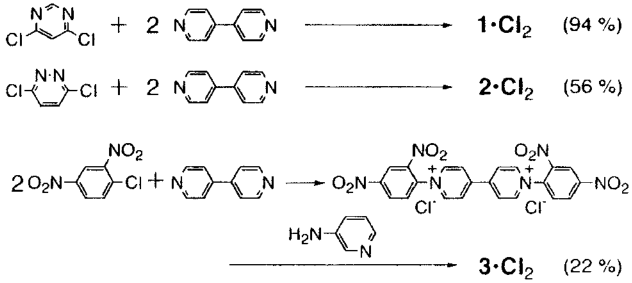

SCHEME 1 Synthetic routes to N-arylpyridinium conjugated ligands

Redox property of the N-arylpyridinium ligands

Redox potentials of **1-3** were evaluated by differential pulse voltammetry using a Hokuto-Denko HZ-3000 potentiostat, equipped with an Ag/AgCl electrodes and a pair of platinum electrodes as reference, working, and counter electrodes, respectively. All these ligands showed two reduction peaks and

TABLE 1. Reduction potentials of N-arylpyridinium ligands.

Ligand	$E_{1/2}$(+2/+1)	$E_{1/2}$(+1/0)
1	**-257 mV**	**-433 mV**
2	**-336 mV**	**-499 mV**
3	**-61 mV**	**-350 mV**
4		**-480 mV**
5	**-690 mV**[6]	**-1120 mV**[6]

Differential pulse voltammograms were obtained in CH_3CN containing 0.1M tetra-n-butylammonium hexafluorophosphate. The obtained potentials are described against Ag/AgCl reference electrode.

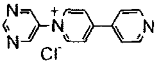

4·Cl

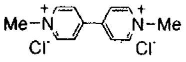

5·Cl$_2$

the reduction potentials were listed in Table 1 together with those of the corresponding monopyridinium derivative **4** and methyl viologen **5** as references. The dimers, **1** and **2**, show stronger electron-deficient properties than the corresponding monomer **1**. The reduction peaks of **3** shifted more cathodically than that of methylviologen **5**. Smaller potential difference between the first and the second peaks of **3** than that of methylviologen may be interpreted by the reduction of on-site Coulombic repulsion due to the extending π-conjugated system by the heteroaromatic substituents.

The reduction processes of **1**-**3** were also monitored by UV-Vis absorption spectra under potentiostatic condition with a Pt-grid working electrode. In the case of meta-pyridylpyridinium-type dimer **1**, the absorbance of the π-π* transition band at 295 nm decreased in the first reduction process with cathodically sweeping potential down to -400 mV, while the 390 nm band, assignable to the one-electron-reduced ion radical,[7] increased with two isosbestic points at 269 and 323 nm. When the second reduction process started from -450 mV, the 390 nm band shifted to 360 nm and a new isosbestic point appeared at 266 nm. In the case of para-pyridylpyridinium-type dimer **2**, the absorbance of the π-π* band at 293 nm decreased in the first reduction process down to -400 mV, while the 367 nm band, assignable to the one-electron-reduced ion radical, increased with two isosbestic points at 269 and

330nm. When the second reduction process started from -450 mV, the 390 nm band shifted to 357 nm with new isosbestic points at 258 and 327 nm. In the case of **3**, the absorbance of the 293 nm band decreased, and the 431 and 643 nm bands, characteristic of its ionradical,[8] increased in the first reduction process down to -300 mV with an isosbestic point at 347 nm. In the second reduction process, both bands disappeared with new isosbestic points at 358 and 472 nm. These spectral behaviors also support the two-step process of the redox property of these ligands.

Photochemical reaction of the ligands in the solid state

The photochemical control of the redox processes of these ligands in the solid state were investigated spectrophotometrically in the reflection-absorption technique suitable for powdered samples. Figure 1 shows the absorption spectral changes of powdered **1**-**3**•Cl_2 under light irradiation.[9] Every spectrum was taken every 5 min. In the case of **1**, the absorbances of two broad absorption bands at 424 and 640 nm increased and the 324 nm band decreased in the first reduction process, and then the 640 and 324 nm bands shifted to 560 and 298 nm, respectively, with monotonous change in both absorbances. This change suggests the successive two-

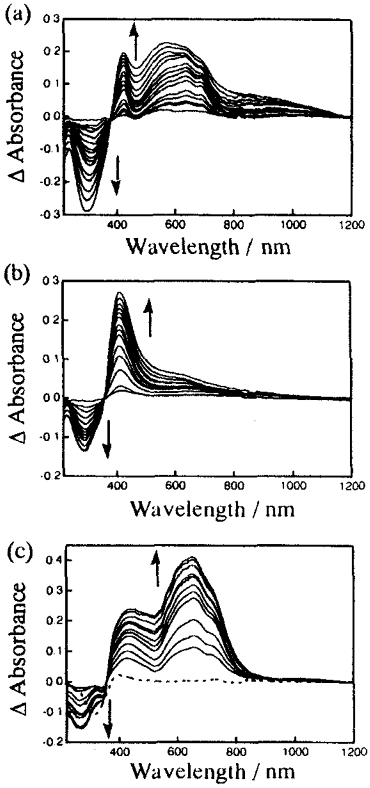

FIGURE 1 Absorption spectral changes of the ligands (a) **1**, (b) **2**, and (c) **3** under light irradiation. Every spectra were taken every 5 min.

step redox process in the solid state under irradiation. In the case of **2**, the absorbance of the absorption band at 414 nm increased while the 296 band *decreased with irradiation time. In the case of* **3**, *the absorbance of two* broad absorption bands at 428 and 660 nm increased while the 264 nm band decreased. The feature of the spectral changes looks similar to that obtained in the solution under potentiostatic condition. However, the relative magnitude of the spectral changes between the parent π–π^* transition and the lowest *energy transition bands are different. The extinction coefficient of the broad* absorption bands around 600 nm in **1** and **3** were quite large in the solid state. This feature was not observed in **2**, although both the excited states would be localized on the pyridylpyridinium moieties. The reason of the enhanced 600-nm bands in **1** and **3** are not clear in the present study and further investigation will be required. The **3**•$(ClO_4)_2$ showed no indication of the ionradical formation even after light-irradiation for 1 hour (the dotted line in Fig. 3c), while the chloride showed quite efficient ionradical formation. This result strongly suggests that the chloride anion acts as the electron donor of the photoinduced electron transfer in the solid state.

Complexation of ligands 1-3

Complexation of the photochemically active ligands **1**-**3** were investigated by self-assembling with various metal ions such as Cu, Fe, Mn, Co, Ni, and Zn in their common solvents. Among them, we obtained single crystals of a coordination polymer, Zn•$\mathbf{3}_2$•$(ClO_4)_6(CH_3CN)_2$, prepared by so-called diffusion crystallization between **3**•$(ClO_4)_2$ and $Zn(ClO_4)_2$ in acetonitrile.[10] As Figure 2 shows, one Zn atom is coordinated by four **3** ligands and two acetonitrile molecules, and their opposite pyridyl moieties coordinate to the neighboring Zn atoms to form the coordination polymer. Namely, four Zn atoms and four bidentate ligands **3** form a coplanar rhombic structure in a unit cell. The crevice of the rhombic skeleton is filled with perchlorate ions as counter anions and acetonitrile molecules as axial ligands, although the structure could not be obtained precisely by disorder. The apexes of the rhombic skeleton (Zn atoms) are shared with the neighboring rhombic skeletons to form 2-

dimensional sheet-like structure.

We found the difficulty to obtain a coordination polymer with these ligands, because the pyridyl moieties of these ligands show weak Lewis basicity, not enough to form a stable coordination polymer, probably because the conjugated pyridinium moieties tend to withdraw π electron density of the pyridyl moieties. For a example, when the $\mathbf{2}\bullet PF_6$ salt was mixed with $CoCl_2$ in acetonitrile, the simple salt of $\mathbf{2}\bullet CoCl_4$ was obtained, resulted from the disproportionation of $CoCl_2$ as shown in Figure 3.[11] In another case, $\mathbf{3}\bullet(CuCl_2)_2$ molecule was obtained as a dark red crystal through the reaction between $\mathbf{3}\bullet Cl_2$ and copper hexafluoroacetylacetonate complex ($Cu\bullet hfac_2$) in methanol, as shown in Figure 4.[12] Although this complex contains metal coordination bond, it has no spin

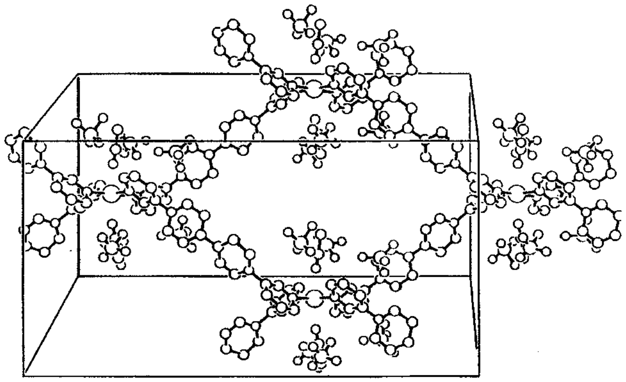

FIGURE 2 PLUTO drawing of the $Zn\bullet\mathbf{3}_2\bullet(ClO_4)_6(CH_3CN)_2$ on the (0 0 1) plane.

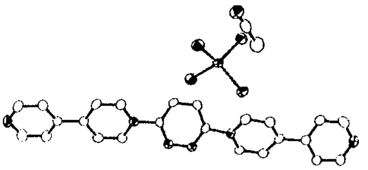

FIGURE 3 ORTEP drawing of the $\mathbf{2}\bullet CoCl_4\bullet CH_3CN$ salt.

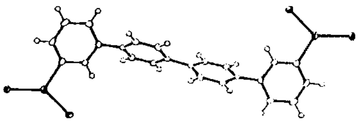

FIGURE 4 ORTEP drawing of the $\mathbf{3}\bullet(CuCl_2)_2$ molecule.

in ESR and SQUID measurements because the Cu is monovalent. The Cu(I) should be obtained through the reduction of Cu(II) with one-electron reduced **3** (**3**$^{+\cdot}$), which could be generated through oxidation of methanol to formaldehyde.[13]

To obtain the photochemically reactive coordination polymer, the Cu•**3**•Cl_4 complex was prepared by the diffusion crystallization of aqueous solutions containing **3**•Cl_2 and $CuCl_2$, according to the complexation method for 4,4'-bipyridine-$CuCl_2$ coordination polymer.[14] The 1:1 composition of the ligand and metal ions was assured by CHN elemental analysis and the ICP measurement.[15] Different from the **3**•$(CuCl_2)_2$ case, this complex showed an ESR signal at g = 2.1074, indicating the included Cu should be divalent. The magnetic susceptibility measurement with a SQUID magnetometer showed paramagnetic behavior with small antiferromagnetic interaction (Weiss temperature = -0.5 K) between the neighboring Cu(II) spins through the conjugated path of the ligand. The Curie constant of 0.377 emu•K•mol^{-1} around 300 K, consistent with the composition of the Cu•**3**•Cl_4 (0.375). After light irradiation for 3 hours, the Curie constant in a high temperature region (around 300 K) increased by about 12 % while the χT value at 2 K decreased 13 %. The increase of the Curie constant at 300 K means the increase of spin concentration due to the formation of viologen ionradical and the decrease of the χT value at 2 K means the the enhancement of the antiferromagnetic interaction between the Cu(II) spins and the photogenerated ionradicals, as shown in Figure 5a. This result suggests that the magnetic interaction between the Cu(II) spins can be controlled photochemically with ligand **3**.

This photochemically active ligand **3** can be applicable to various light-tunable spin systems. For a example, if the Cu(II) ion is replaced by other metal ions with higher spin multiplicity (>2/2), such as Ni(II), Mn(II), and so on, the ferrimagnetic spin alignment would be realized in the complex after light irradiation as shown in Figure 5b, depend on the alternating one-dimensional structure of the metal ions and the ligand. On the other hand, if the complex take the similar two-dimensional sheet-like structure as Zn•$\mathbf{3}_2$•$(ClO_4)_n(CH_3CN)_2$ complex, the complex will also show the ferrimagnetic spin alignment after light irradiation. Thus the photochemically active ligand can be utilized to develop various photofunctional magnetic properties depend on the complex structure and the spin multiplicities of the metal ions.

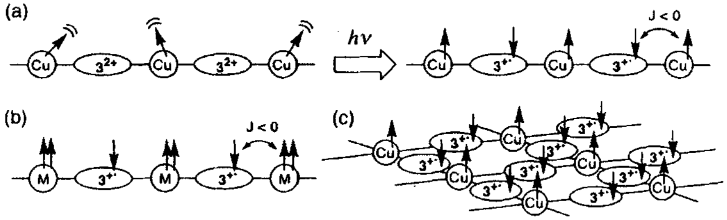

FIGURE 5 Possible spin-exchange interaction in the metal-complexes of ligand **3** with (a) one-dimensional alternating chain structure, (b) one-dimensional alternating chain with higher spin metal, and (c) two dimensional structure.

CONCLUSION

N-aryl pyridinium molecules, 4,6-bis(4,4'-bipyridine-1-yl)-pyrimidine (**1**), 3,6-bis(4,4'-bipyrdine-1-yl)-pyridazine (**2**), and 3-pyridyl viologen (**3**) were synthesized as photoelectrochemically tunable ligands. They exhibited two step successive absorptional changes due to the two-step reduction processes under electrochemical reduction and light irradiation. Especially, the Cu(II) complex of **3** showed the increase of the spin concentration upon light irradiation and the antiferromagnetic interaction between the light-generated ionradical and Cu(II) spins. Thus the N-arylpyridinium ligands have large possibility to develop novel assembly functions.

Acknowledgments

This work was partially supported by Grant-in-Aid for Scientific Research (A) (No. 11305061), and Scientific Research on Priority Areas of "Electrochemistry of Ordered Interfaces" (No.282/09237256) and "Development of Molecular Conductors and Magnets by Spin-Control"

(No.730/11224207) from the Ministry of Education, Science, Sports, and Culture, Japan. The authors also acknowledge the financial support of Tokuyama Science Promotion Foundation.

References

[1] H. Dúrr, H. Bouas-Laurent, *Eds., Photochromism Molecules and Systems* (Elsevier, Amsterdam, 1990).

[2] P. M. S. Monk, *The Viologens* (Jhon Wiley & Sons, Chichester, 1998).

[3] T. W. Ebbesen and G. Ferraudi, *J. Phys. Chem.*, **87**, 3717 (1983).

[4] M. M. Matsushita, T. Tachikawa, T. Suzuki, T. Kawai, and T. Iyoda, *Mol. Cryst. Liq. Cryst.*, **334,** 149–156 (1999).

[5] J. G. Allen, I. C. I. Ltd, B.P. 1399595, App. No. 18535/71, 1975.

[6] C. Bird and A.T. Kuhn, *Chem. Soc. Rev.,* **10,** 49–82, (1981).

[7] E. M. Kosower, E. J. Land, and A. J. Swallow, *J. Am. Chem. Soc.*, **94,** 986–987 (1972).

[8] E. Kosower and J. L. Cotter, *J. Am. Chem. Soc.*, **86,** 5524 (1964).

[9] The light irradiation were performed with a 150 W Xenon lamp. The light intensity on the sample was 1300 μW/cm above through no filter ($\lambda > 300$ nm).

[10] Crystal data for $Zn{\bullet}3_2{\bullet}(ClO_4)_6(CH_3CN)_2$ ($C_{44}H_{38}N_{10}O_{24}Cl_6Zn$): *monoclinic, C2/c,* a = 15.465 (6) b = 29.225 (9), c = 19.171 (5) Å, β = 108.40(2)°, V = 8221.8 (42) Å^3, Z = 8, R =0.235, unique reflection data ($\sigma > 3$), 3923. The R value is not enough small to figure out the precise structure because of low quality of the obtained crystals in which the incorporated acetonitrile molecules tend to be released from the crystal and then crystal was collapsed. Further investigation will be required.

[11] Crystal data for $2{\bullet}CoCl_4{\bullet}CH_3CN$ salt ($C_{24}H_{18}N_6CoCl_4$): *monoclinic, $P2_1/a$,* a = 17.245 (4), b = 21.250 (4), c = 7.442 (2) Å, β = 95.31 (2)°, V = 2715.4 (9) Å^3, Z = 4, R = 0.044, unique reflection data ($\sigma > 3$), 2796.

[12] Crystal data for $3{\bullet}(CuCl_2)_2$ ($C_{20}H_{16}N_4Cl_4Cu_2$): *monoclinic, C2/c,* a = 22.509 (3), b = 6.5559 (8), c = 14.3191 (17) Å, β = 99.345(3)°, V = 2085.0 (4) Å^3, Z = 4, R = 0.033, unique reflection data ($\sigma > 2$), 2582.

[13] J. A. Farrington, A. Ledwith and M. F. Stam, *J. Chem. Soc., Chem. Commun.* **1969,** 259.

[14] N. Masciocchi, P. Cairati, L. Carlucci, G. Mezza, G. Ciani, and A. Sironi, *J. Chem. Soc., Dalton Trans.*, **1996,** 2739–2746.

[15] E.A. calcd for $C_{20}H_{18}Cl_4CuN_4O$ ($3{\bullet}Cu{\bullet}Cl_4{\bullet}H_2O$): C, 44.84; H, 3.39; N, 10.46 %. Found: C, 44.82; H, 3.57; N, 10.24 %.